/N-39
96730
P. 12

STRUCTURAL DYNAMIC INTERACTION WITH SOLAR TRACKING CONTROL FOR EVOLUTIONARY SPACE STATION CONCEPTS

Tae W. Lim, Paul A. Cooper, and J. Kirk Ayers

May 1992

NASA

National Aeronautics and
Space Administration

Langley Research Center
Hampton, Virginia 23665

STRUCTURAL DYNAMIC INTERACTION WITH SOLAR TRACKING CONTROL
FOR EVOLUTIONARY SPACE STATION CONCEPTS

Tae W. Lim[*]
Lockheed Engineering and Sciences Company
Hampton, Virginia

Paul A. Cooper[**]
NASA Langley Research Center
Hampton, Virginia

and

J. Kirk Ayers[+]
Lockheed Engineering and Sciences Company
Hampton, Virginia

Abstract

This paper addresses the sun tracking control system design of the Solar Alpha Rotary Joint (SARJ) and the interaction of the control system with the flexible structure of Space Station Freedom (SSF) evolutionary concepts. The significant components of the space station pertaining to the SARJ control are described and the tracking control system design is presented. Finite element models representing two evolutionary concepts, Enhanced Operations Capability (EOC) and Extended Operations Capability (XOC), are employed to evaluate the influence of low frequency flexible structure on the control system design and performance. The design variables of the control system are synthesized using a constrained optimization technique to meet design requirements, to provide a given level of control system stability margin, and to achieve the most responsive tracking performance. The resulting SARJ control system design and performance of the EOC and XOC configurations are presented and compared to those of the SSF configuration. Performance limitations caused by the low frequency of the dominant flexible mode are discussed.

Introduction

Evolutionary concepts of the space station employ photovoltaic (PV) solar arrays and solar dynamic (SD) units which track the sun during orbital daylight to obtain electric power. PV arrays convert solar energy into electrical power using a large number of solar cells and the SD units produce electricity by supplying solar energy to a working fluid which operates an electricity generator. In the current design, the PV arrays are attached to deployable masts which are in turn attached through a rotary joint, called a Solar Beta Rotary Joint (Beta Joint), to the outboard portion of transverse booms. Similarly, the SD units are attached to the outboard transverse booms through a rotary joint called a Beta Gimbal. The Beta Joint and Beta Gimbal permit rotation of the arrays and SD units, respectively, to compensate for the seasonal variation of the orbit plane with respect to the ecliptic plane. Rotary joints, called Solar

---

[*] Senior engineer, member AIAA.
[**] Senior engineer, Spacecraft Dynamics Branch, associate fellow AIAA.
[+] Senior engineer.

Alpha Rotary Joints (SARJ or Alpha Joints), regulate the relative rotational position of the outboard structure to the inboard structure. The attitude of the inboard structure is controlled by Control Moment Gyros (CMG's) and Reaction Control System (RCS) jets. The Alpha Joints are used to orient the PV array surface and SD concentrator normal vectors along the solar vector so that maximum solar energy may be obtained during the daylight portion of each orbit. The Alpha Joint control is designed to be a basic position tracking system with minor-loop velocity feedback to stabilize and provide damping to the rigid body tracking motion. A proportional-integral (P-I) compensation is added in both the velocity and position loops to minimize steady-state tracking error.[1]

The allowable control bandwidth of the proposed SSF Alpha Joint controller[2] encompasses the resonant structural frequencies of the outboard boom and the PV and SD systems so that the possibility for adverse interaction between the rigid body control system and the elastic response of the structure exists. To compensate for the possible undesirable effect of control/structure interaction, a low pass filter is added to the velocity loop to attenuate the structural response signal. The proper placement of the corner frequency of the filter and selection of values for gain setting of the P-I compensation in the velocity and position loops are required to provide optimum performance. Selection of the proper filter and gain settings depends on the accuracy of the predictions of the structural frequencies and modal response at sensor and actuator locations. Since the space station configurations are too large and flexible to support their weight on earth, the structural dynamic characteristics will have to be estimated from analytical models and component modal tests rather than from modal tests of the actual assembled structures. Because of the considerable uncertainty involved in predicting the dynamic characteristics of the station, the solar tracking control system should be designed with a high degree of stability robustness to assure stable tracking for a range of variation in structural parameters possible due to configuration changes and errors in analytical estimation. The objective of this paper is to investigate how the increased rigid body inertia and the reduced fundamental structural resonant frequencies of the evolutionary space station concepts influence the stability and performance of the solar tracking control system.

Assuming that the station is maintained at a local-vertical-local-horizontal (LVLH) attitude, the Alpha Joint rotation rate would be the orbital rate, completing a revolution approximately every 90 minutes. The LVLH X-axis is parallel to the flight direction, the LVLH Z-axis is directed to the nadir, and the LVLH Y-axis is orthogonal to

the orbit plane. The rotation of the Beta Joint is extremely slow over an orbit and follows the yearly variation of the orbit plane. Since the Beta Joint motion is slow and the primary sun tracking function is performed by the Alpha Joint, the Beta Joint drive and control system are not addressed in this study.

This paper is organized as follows: First, the significant components of the space station related to the Alpha Joint control are depicted and the sun tracking control system is described. Then, the procedure of synthesizing the control design variables is addressed. The synthesis procedure employs constrained optimization techniques to meet the SSF design requirements, to provide a given level of stability margin, and to obtain the most responsive tracking possible consistent with the assumed structural characteristics. Finally, simulation results using the optimized design variables are presented.

Description of SSF evolutionary concepts, Alpha Joint, and sun tracking function

Description of SSF evolutionary concepts

The space station structure can be broadly divided into an inboard core structure and an outboard articulating structure. As shown in Fig. 1, the inboard core structure of SSF is comprised of a module cluster, center truss, thermal control system (TCS) radiators, and various user payloads. The port and starboard truss, PV arrays and electrical power system (EPS) radiators constitute the outboard articulating structure and will be referred to as the outboard structure. The Alpha Joint connects the inboard and outboard structures and provides a means for relative rotation of the outboard structure with respect to the inboard structure.
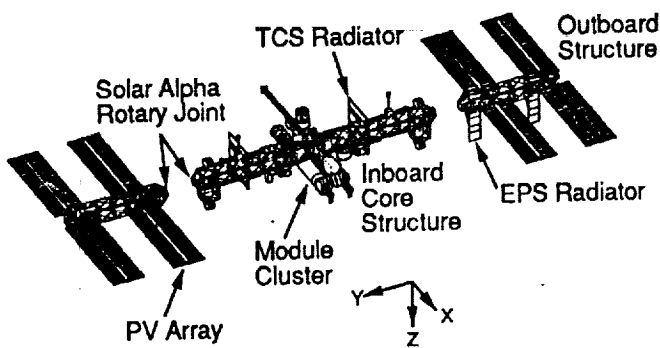
Two SSF based evolutionary concepts are shown in Figs. 2 and 3. The Enhanced Operations Capability (EOC) configuration includes dual keels and upper and lower booms on the center truss, an additional module, increased thermal radiation capacity, and an extended outboard truss with SD units for increased power generation capability. The EOC configuration is designed to provide enhanced research and development capability, and support initial Space Exploration Initiative (SEI) activities. The Extended Operations Capability (XOC) configuration is an augmented version of the EOC configuration with additional SD units on extended outboard truss booms, an additional module and pocket laboratories, increased thermal radiation capability, and a lunar vehicle assembly/servicing facility. The XOC configuration is tailored to support assembly and verification of reusable lunar vehicles, and life science research required to facilitate a SEI Mars mission.

Physical description of Alpha Joint

Each Alpha Joint consists of dual motors, dual resolvers, a motor controller, drive pinions, a bull gear and trundle bearings as depicted schematically in Fig. 4.[3] The motor provides the torque required to rotate the outboard structure. The amount of control torque provided by the motor is determined by the motor controller based on the measurements obtained by the joint resolver and the desired rotation data from the Velocity Vector Generator (VVG) on the station. The motor drive pinion to bull gear ratio has been selected to minimize mechanical parts count and hence maximize reliability.[4] The bull gear is rigidly attached to the outboard structure through a shear plate.
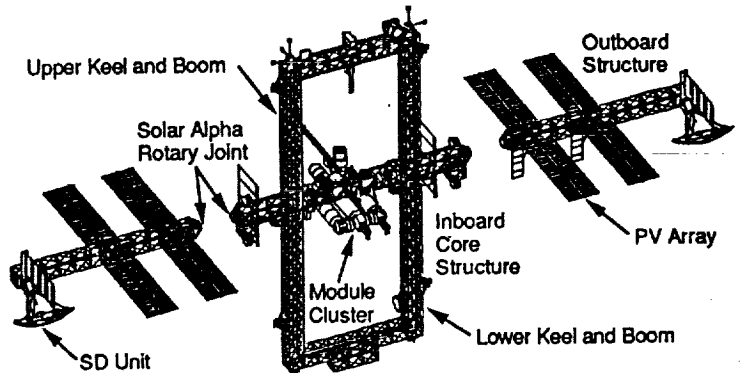

Fig. 1 SSF Assembly Complete configuration

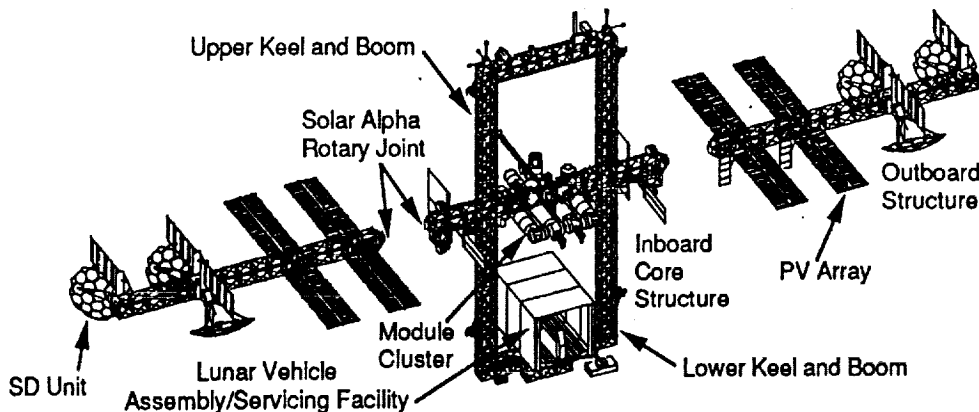Fig. 2 Enhanced Operations Capability configuration

Fig. 3 Extended Operations Capability configuration

2

The large bull gear (about 10 foot diameter) is equipped with trundle bearings in order to accommodate large temperature gradients. The trundle bearings are the main source of friction. A set of high power roll rings (not shown in Fig. 4) carries electrical power across the joint as the joint rotates.[4]
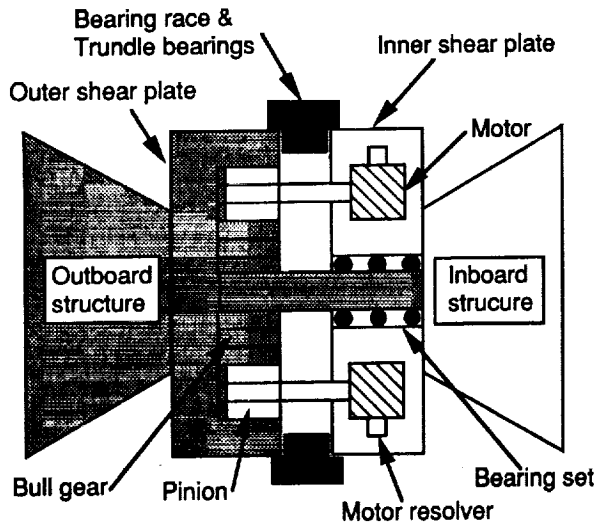

Fig. 4 Sketch of Alpha Joint drive train

Description of sun tracking control system

The SARJ motor controller generates the required motor torque based on the difference between the desired and measured relative joint position and velocity at points A and B as shown in Fig. 5. Point A is fixed to the inboard structure while point B is located on the outboard structure. The desired relative joint velocity command is determined by the VVG on the station and is an input to the SARJ motor control system. As the SARJ position leads or lags the desired position (also provided by the VVG), the velocity

command is increased or decreased to compensate for the position error. Hence the reference input to the control system includes the desired relative angular velocity (ω_B - ω_A) and the desired relative angular position (θ_B - θ_A).
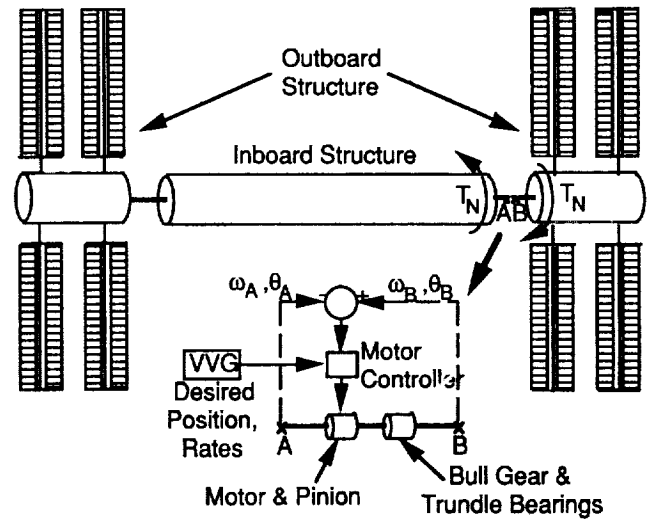

Fig. 5 Schematic of Alpha Joint control system

The detailed control system used in this study is based on the design obtained from the SSF Preliminary Design Review document.[2] A block diagram of the control system is shown in Fig. 6. The control system consists of an inner velocity servo loop and an outer position servo loop. The input to the velocity loop is a summation of the desired joint velocity and the position error. The position loop enhances the tracking performance by increasing or decreasing the velocity command depending upon the position error. The velocity command is converted to a voltage command and the maximum allowable SARJ velocity is constrained by a voltage limiter.
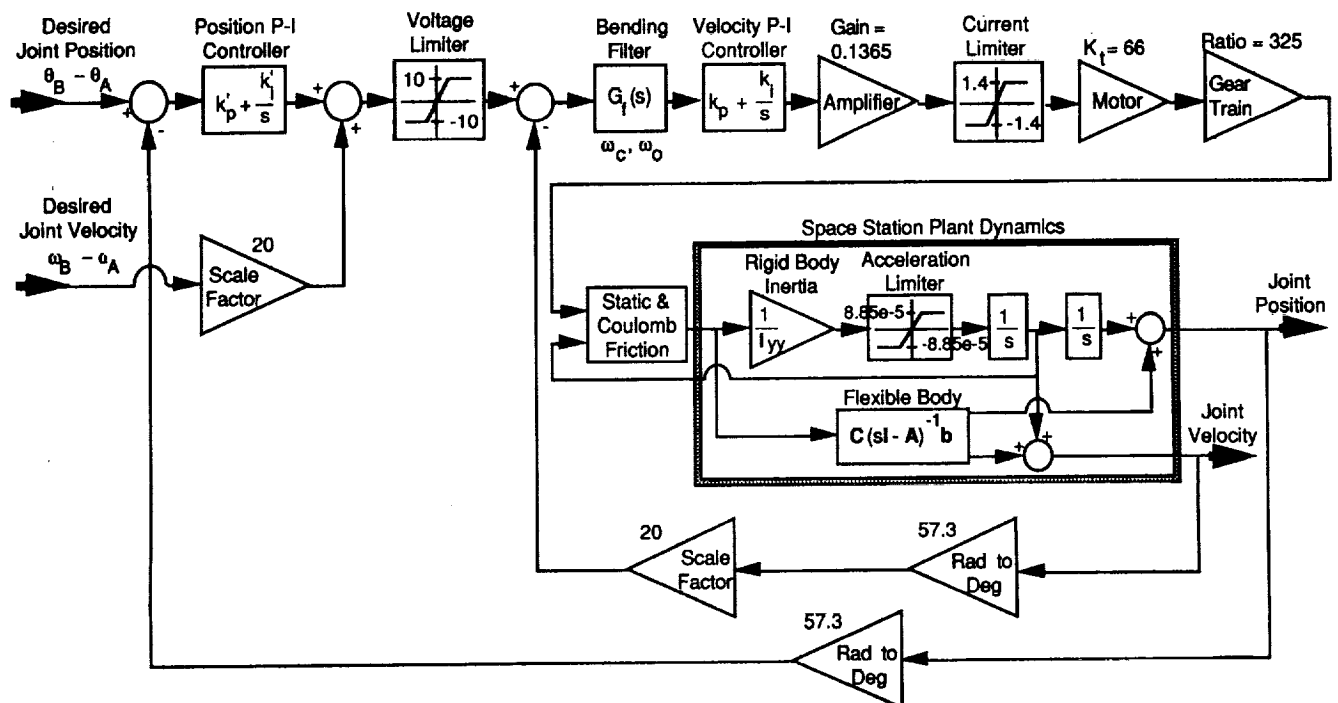

Fig. 6 Block diagram of Solar Alpha Rotary Joint Controller

3

The inner servo loop includes a fourth order Butterworth bending filter[5] to roll-off the flexible structural response in the signal. Two additional zeros are included in the filter to reduce the loss of phase margin due to phase shift. The filter corner frequency (ω_c) and the frequency of the zeros (ω_0) are design parameters. The transfer function of the bending filter is

$$G_f(s) = \frac{\omega_c^4 (\frac{s^2}{\omega_0^2} + \frac{1.4s}{\omega_0} + 1)}{s^4 + 2.6131\omega_c s^3 + 3.4142\omega_c^2 s^2 + 2.6131\omega_c^3 s + \omega_c^4} \quad (1)$$

While the proportional control in the inner loop increases system damping, it produces a steady-state tracking error for a ramp input. The introduction of integral control helps to reduce steady state errors. Therefore, a proportional-integral (P-I) controller is used for the inner velocity loop and a similar P-I controller is used for the outer position loop. The position loop has a double integrator (one in the outer loop and the other in the inner loop) to track a ramp signal with zero steady state error. The P-I controllers are also provided with integration limits to prevent the system from being overdriven.[2] This is required due to the acceleration limits imposed on the SARJ. Each P-I controller has two gain settings: K_p and K_i are the proportional and integral gains for the velocity loop, and K'_p and K'_i are the corresponding gains for the position loop. These four gains are also included as design parameters.

The power amplifier shown in Fig. 6 is equipped with a current limiter. A 66 in-lbf/amp motor torque constant and a gear ratio of 325 is assumed.[2] The output torque from the gear is subject to the large static and dynamic friction torques of the trundle bearings. The output torque must exceed the static friction torque to initiate the motion of the SARJ. Once the motion is initiated, a net torque, which is the motor torque subtracted by the dynamic friction, is applied to the structure at point B (actuator point) as shown in Fig. 5. The estimated magnitudes of joint static and dynamic friction torques are 3580 in-lbf and 2870 in-lbf, respectively.[2]

Space station plant dynamics model for Alpha Joint control study

The space station structure is modelled using finite element techniques. The finite element models of the SSF configurations were created to investigate the influence of elastic response on the Alpha Joint control system design and performance. Two coincident grids were placed at the center node of the SSF Alpha Joint as indicated in Fig. 7, to provide a rotational degree-of-freedom (DOF) about the Y-axis of the outboard structure. These grids are rigidly connected in the other five DOF. Then the undamped natural frequencies and mode shapes of the finite element model were computed. The finite element models have eight rigid body modes. The EOC and XOC finite element models were generated in the same manner.

The undamped natural frequency distribution of the SSF, EOC, and XOC configurations below 2 Hz is shown in Fig. 8. Including the eight rigid body modes, there are 148, 185, and 242 modes below 2 Hz for the SSF, EOC, and XOC configurations, respectively. The modal density is
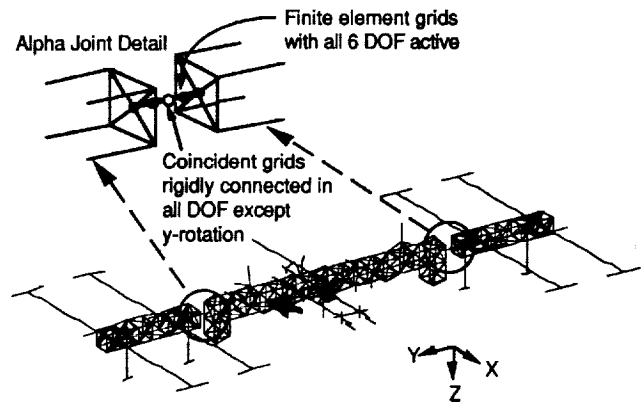

Fig. 7 Finite element model of Space Station Freedom

increased significantly as more structure is added to EOC and XOC. Since the rotational rate of the outboard structure is at the order of the orbital rate, i.e., approximately 0.0002 Hz, and is much smaller than the minimum control bandwidth of 0.01 Hz, it is assumed that the plant model is time-invariant and the dynamic influence due to the articulation of the Alpha Joint is negligible for the purpose of the investigation addressed in this paper.
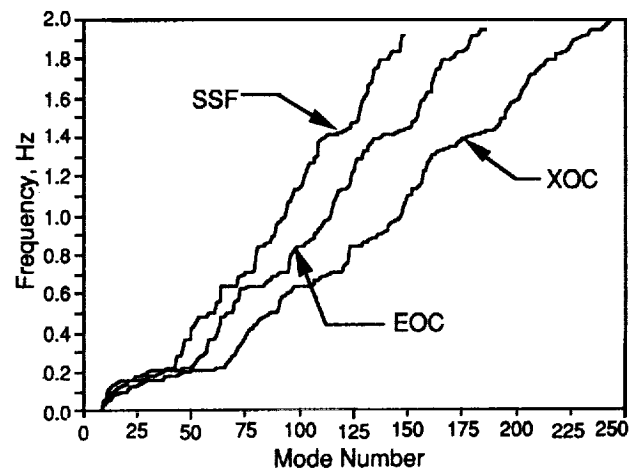

Fig. 8 Comparison of evolutionary configuration natural frequencies below 2 Hz

The state-space equation governing the flexible response at the port SARJ is represented by

$$\dot{x} = Ax + bu$$
$$y = Cx \quad (2)$$

where

$$x = \begin{Bmatrix} q \\ \dot{q} \end{Bmatrix}, \quad A = \begin{bmatrix} 0 & I \\ -\Omega^2 & -2Z\Omega \end{bmatrix}, \quad b = \begin{Bmatrix} 0 \\ \phi_B^T \end{Bmatrix}$$

$$y = \begin{Bmatrix} \theta_B - \theta_A \\ \omega_B - \omega_A \end{Bmatrix}, \text{ and } C = \begin{bmatrix} \phi_B - \phi_A & 0 \\ 0 & \phi_B - \phi_A \end{bmatrix}$$

4

where q is the modal displacement vector; θ_A and θ_B are the angular displacements at the points A and B, respectively; ω_A and ω_B are the angular velocities at the points A and B, respectively; Ω = diag$\{\omega_i\}$ and Z = diag$\{\zeta_i\}$ in which ω_i and ζ_i are the natural frequency and modal damping ratio of the ith flexible mode, respectively; ϕ_A and ϕ_B are the row vectors of the unity mass normalized mode shape matrix corresponding to the Y-rotational DOF at the points A and B, respectively. A modal damping ratio of 0.1% is assumed for all the flexible modes as a baseline value for the design synthesis and simulation of the SARJ control system.

The state-space flexible structure model is combined with the rigid body model to characterize the dynamics of the space station structure. The rigid body model represents the inertia property of the outboard structure with respect to the Alpha Joint rotational axis, i.e., Y-axis. Table 1 shows the inertia properties of the outboard structure for either starboard or port side of the SSF, EOC and XOC configurations. The net torque (T_N) applied to the structure at actuator point B (Fig. 5) causes motion of the flexible structure. The actual joint position and velocity containing both rigid body and elastic components are measured and fed back to close the control system loops.

Table 1 Rigid body inertia properties of outboard structure (port or starboard)

Configuration	I_{yy} (lb-in-sec^2)	% increase over SSF
SSF	1.75×10^7	0.0
EOC	2.37×10^7	35.4
XOC	3.79×10^7	116.6

Synthesis procedure of control system design variables

Control system requirements

The SARJ control system discussed earlier has six design variables to be selected to optimize control system performance and to satisfy prescribed design requirements. Table 2 summarizes the design objective, the design variables, and the design constraints. The design constraints can be classified as either frequency-domain or time-domain constraints. The frequency-domain constraints in both inner and outer loops are as follows: (1) Rigid body open-loop gain and phase margins must be greater than or equal to 6 dB and 45 degrees, respectively, to assure a stable rigid body motion; (2) The closed-loop poles associated with the rigid body and controller should have a minimum damping ratio of 0.5. By constraining rigid body and controller closed-loop poles to a prescribed sector in the complex plane, this frequency-domain constraint assures low overshoot in the transient response in the time-domain; (3) Apparent gain margin, defined as the minimum distance of the open-loop gain from the zero dB line in the frequency range encompassing the structural resonance frequencies, should be at least 20 dB to guarantee enough stability margin to compensate for uncertainties in the plant. The frequency-domain constraints are not requirements of the Space Station program. They are imposed for the investigation in this paper. The time-domain constraints include small steady-state pointing errors and low jitter. The jitter is defined as the peak-to-peak variation of the position error in one second. The time-domain constraints are required by the SSF Preliminary Design Review document.[2]

The Preliminary Design Review document also requires that the inner (velocity) and outer (position) closed-loop bandwidths (BWv & BWp) be between 0.01 and 1 Hz. This requirement is treated as part of a performance index which is to be maximized. The bandwidths are a measure of the responsiveness of control system and also represent disturbance rejection thresholds. The other component of the performance index to be maximized is the magnitude of the absolute real part of the dominant rigid body and controller closed-loop pole (σ). The dominant pole is defined here as the rigid body and controller closed-loop pole (for both inner and outer loops) closest to the imaginary axis. This second component of the performance index is imposed in order to minimize settling time in a time-domain analysis.

Modeling of space station dynamics

The plant model includes the rigid body inertia of the outboard structure about the Alpha Joint axis and the flexible modes. Figure 9 shows a frequency response function (FRF) of the flexible body with all flexible modes of the finite element model up to a frequency of 2 Hz at the port Alpha Joint with the station configuration in the minimum drag PV orientation. The FRF shown is the magnitude ratio of the velocity response at the port Alpha Joint to net torque applied. To investigate the changes in response characteristics as the outboard structure rotates, the FRF of the SSF port Alpha Joint with the maximum drag PV orientation was evaluated. The differences in FRFs for the two PV orientations are negligible at the dominant mode frequencies. Thus, the plant model for the Alpha Joint is considered time-invariant. Also, the port and starboard

Table 2 Summary of Alpha Joint controller design objective, variables, and constraints

| Design objective	Maximize position and velocity loop bandwidths while minimizing settling time
Design variables	Controller gains (k_p , k_i , k_p' , and k_i') Compensation filter break and zero frequencies (ω_c and ω_o)
Constraints	Rigid body gain margins $\geq$ 6 dB Rigid body phase margins $\geq$ 45 deg Apparent gain margins in structural resonant frequency range $\geq$ 20 dB Minimum rigid body and controller damping ratio $\geq$ 0.5 Bandwidth: between 0.01 and 1 Hz Steady-state pointing accuracy: better than 0.58 deg Jitter $\leq$ 0.01 deg/sec
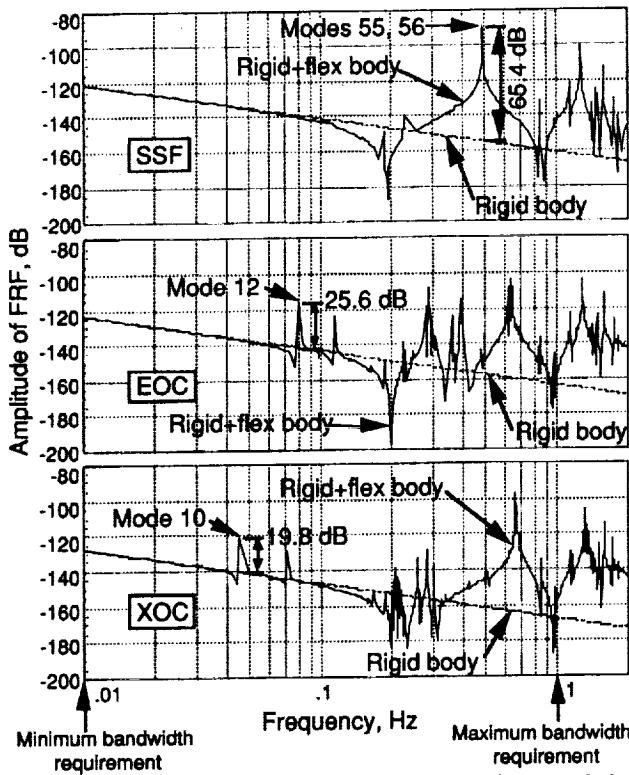
Fig. 9 Comparison of frequency response characteristics

Alpha Joints exhibit similar dynamic response characteristics. Therefore, for this study, the port Alpha Joint with minimum drag orientation is used as a representative plant model.

A control system designed with only the rigid plant taken into account could become unstable if the response signals from the dominant flexible modes are not well attenuated by the control system. The dominant flexible modes (or dominant modes) are the most influential modes among the flexible modes in determining the apparent gain margin. Figure 9 indicates that the dominant flexible modes for SSF occur at frequencies of 0.485 Hz and 0.486 Hz. The frequencies of the dominant modes for EOC and XOC are much lower at 0.081 Hz and 0.044 Hz, respectively. As additional SD units are added to the outboard structure for EOC and XOC, the frequencies of the dominant modes approach the required minimum bandwidth increasing the possibility of adverse interaction between the rigid body controller and the flexible structure.

The mode shapes of the dominant modes are shown in Fig. 10. The dominant mode for SSF corresponds to a rigid body rotation of the outboard trusses coupled with bending of the PV arrays. The dominant modes for EOC an XOC represent the transverse boom bending combined with the torsion of the outboard structure. Other modes which might interfere with rigid body controllers are at higher frequencies. Their influence would be attenuated further by any low pass filter used to roll-off the effects of the dominant modes and can hence be ignored during the control system design. If a notch filter was used rather than the low pass filter to attenuate the dominant mode effects, the modes at the higher frequencies might still interfere with the rigid body controller.

Synthesis procedure

To simplify the synthesis procedure, the limiters in the control system are ignored. The friction block is assumed to have a transfer function of unity, which is a conservative assumption for robust design. The linearized block diagram is shown in Fig. 11. The linearized control system is employed to perform design synthesis using a constrained optimization scheme. It is desirable that the flexible modes
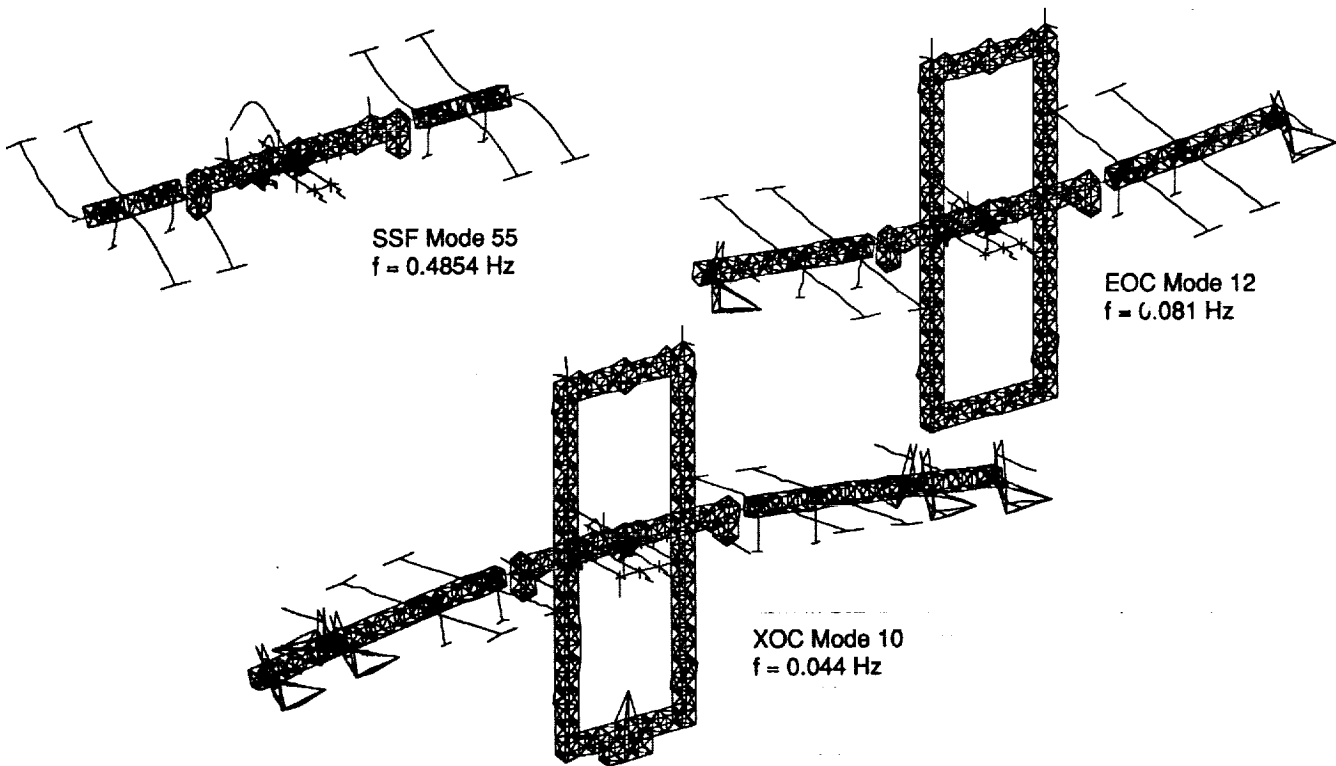

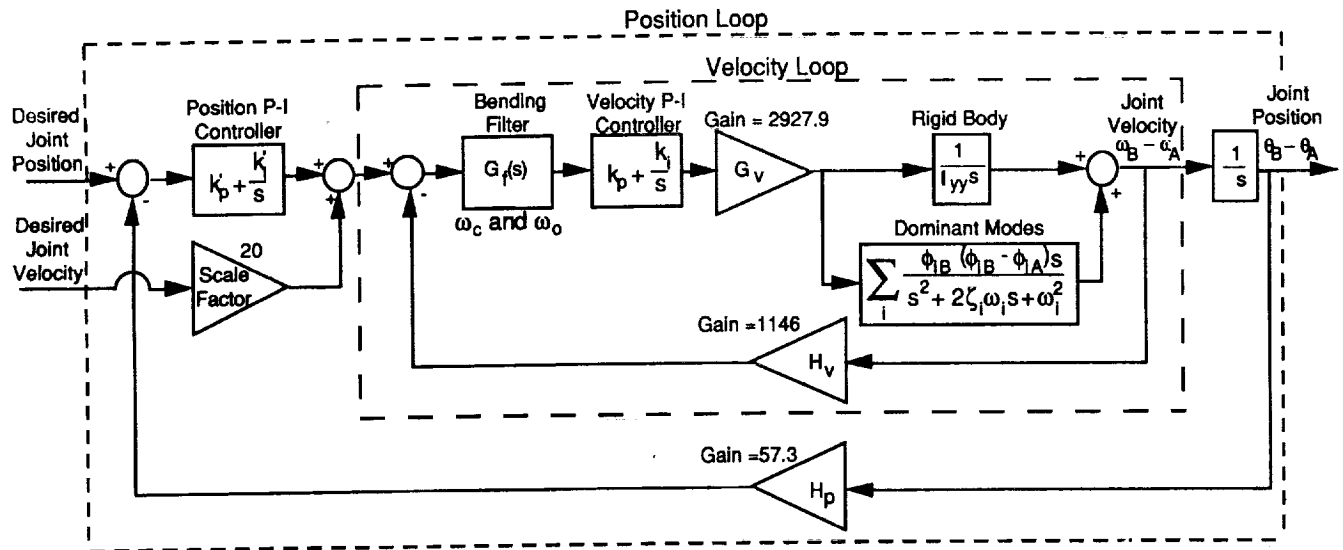Fig. 10 Dominant modes for Alpha Joint control

Fig. 11 Linearized block diagram of Solar Alpha Rotary Joint controller

be removed from the plant during the synthesis of design variables to ease the computational load. For SSF, the dominant flexible modes have a gain of approximately 65.4 dB above the rigid body gain (Fig. 9). Hence the 20 dB apparent gain margin constraint for the plant with the flexible modes is equivalent to a constraint of having a gain less than -85.4 dB for the rigid body plant at the frequency of 0.49 Hz. For the synthesis of design variables, the plant is considered as a rigid body with one of the constraints modified as described above. This consideration is used only for design purposes and not for subsequent frequency response analyses or time response simulations. Similarly, for EOC and XOC, the apparent gain margin constraints are modified. The apparent gain margin constraints for EOC and XOC become 45.6 dB at 0.081 Hz and 39.8 dB at 0.044 Hz, respectively.

The synthesis problem is stated as follows: Find values for the six design variables (ω_c, ω_o, k_p, k_i, k'_p, and k'_i) which maximize the performance index

$$J = \mu_1 BW_v + \mu_2 BW_p + \mu_3 \sigma \qquad (3)$$

while satisfying the constraints

1) Velocity open-loop rigid body gain margin $\geq$ 6 dB
2) Position open-loop rigid body gain margin $\geq$ 6 dB
3) Velocity open-loop rigid body phase margin $\geq 45°$
4) Position open-loop rigid body phase margin $\geq 45°$
5) Minimum rigid body position and velocity closed-loop damping factor ≥ 0.5
6) For SSF, velocity open loop gain at 0.49 Hz $\leq$ -84.5 dB
    For EOC, velocity open loop gain at 0.081 Hz $\leq$ -45.6 dB
    For XOC, velocity open loop gain at 0.044 Hz $\leq$ -39.8 dB

The scalars μ_1, μ_2 and μ_3 are weighting factors. Equal weights of unity are used for μ_1 and μ_2 since the velocity and position closed-loop bandwidths are of equal importance. The magnitude of σ is an order less than the bandwidths expressed in rad/sec. To give approximately equal importance to the settling time, μ_3 = 10 is selected.

The constrained optimization problem is solved using a nonlinear programming method implemented in MATRIXx software.[6] The constrained nonlinear optimization problem is initially approximated by a constrained linear optimization problem with an augmented Lagrangian objective function. Then, sequential quadratic programming is implemented to solve the optimization problem using objective functions approximated to second order. The software uses a recent extension of the Karmarkar's interior point algorithm to solve the resulting quadratic programming problem. The resulting optimized design variables with performance index and constraints are summarized in Table 3. The design results for SSF are taken from Ref. 7. The design for SSF and EOC satisfies all the prescribed design requirements. The position loop bandwidth of EOC is only marginally larger than the minimum design requirement and the position loop bandwidth design for XOC does not meet the SSF design requirement. As the frequencies of the dominant modes decrease for EOC and XOC, the corner frequency of the Butterworth filter is forced to decrease in order to meet the apparent gain margin constraint. The reduced bandwidths obtained for EOC and XOC indicate that the response of the EOC and XOC Alpha Joints will be sluggish compared to that of the SSF Alpha Joint. If the SSF bandwidth requirement is enforced for XOC, the SSF PDR Alpha Joint controller design may not be applicable. A revised controller design employing more sophisticated control/structure interaction techniques may need to be investigated. However, it is logical to believe that, as the evolutionary space station increases in size, the bandwidth requirement will be reduced.

It was noticed that there existed more than one local minimum for the optimization problem so that selection of the initial guess values for the six design variables was important in obtaining the "best" local minimum. However, one cannot be guaranteed that this "best" local minimum obtained is the global minimum. The steady-state time domain requirements listed in Table 2, which were not enforced during the optimization, were checked for violation using the optimized design variables through time response simulation. The following section discusses the design results in detail.

Table 3 Comparison of Alpha Joint controller design results

|	Description	Requirements of SSF	Optimized results		
			SSF	EOC	XOC
Design objectives	Velocity loop bandwidth (BWv, Hz)	$0.01 \leq BWv \leq 1$	0.053	0.021	0.014
	Position loop bandwidth (BWp, Hz)	$0.01 \leq BWp \leq 1$	0.027	0.0105	0.0074*
	Distance of dominant pole to imaginary axis	N/A	0.026	0.0082	0.0018
Design variables	ω_c (rad/sec)	N/A	0.54	0.22	0.15
	ω_o (rad/sec)	N/A	3.83	0.71	0.84
	k_p	N/A	0.73	0.39	0.40
	k_I	N/A	0.016	0.0035	0.00070
	k'_p	N/A	1.07	0.46	0.34
	k'_i	N/A	0.023	0.0031	0.00072
Design constraints	Rigid body velocity loop gain margin (dB)	≥ 6	7.5	8.5	7.9
	Rigid body position loop gain margin (dB)	≥ 6	7.6	8.2	7.8
	Rigid body velocity loop phase margin (deg)	≥ 45	45.0	49.1	53.3
	Rigid body position loop phase margin (deg)	≥ 45	45.1	47.3	52.2
	Velocity loop apparent gain margin (dB)	≥ 20	20.0	21.0	21.0
	Minimum rigid body and controller damping ratio	≥ 0.5	0.51	0.50	0.51

* Violated the SSF design requirements
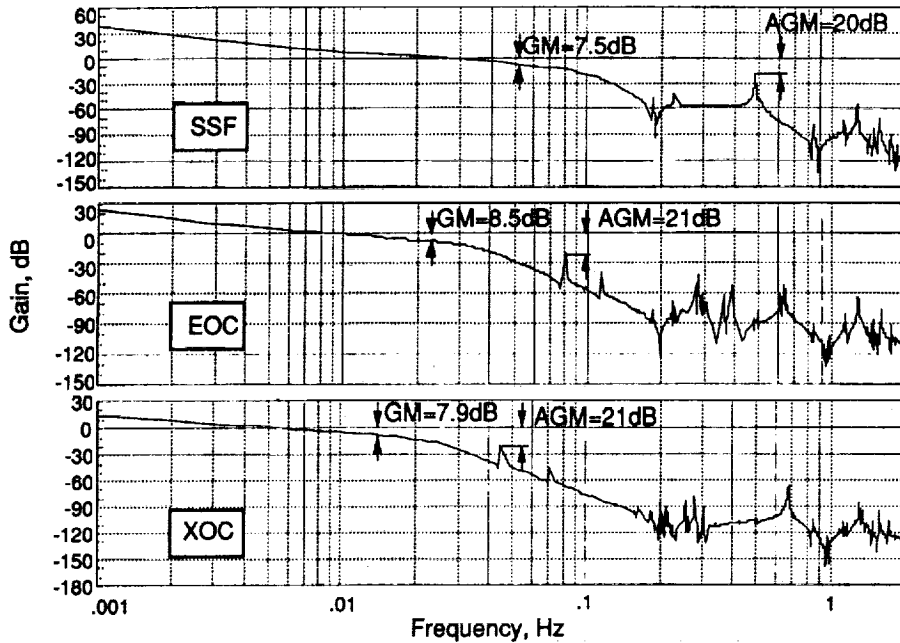
Fig. 12 Comparison of compensated Bode gain plots of port velocity open loop

Design synthesis and simulation results

The compensated Bode plots of the linearized velocity loop on the port side of the station are shown in Figs. 12 and 13. All the flexible modes below 2 Hz were incorporated in the simulation. The constraints of rigid body gain and phase margins, and apparent gain margin in the region of structural resonance frequencies are satisfied as indicated in the figures.

The time response of the control system is simulated for a step velocity command of 4 deg/min and a ramp position command with a slope of 4 deg/min. Figures 14 through 19 show the results of the simulation. All limiters and joint friction as modeled in Fig. 6 are
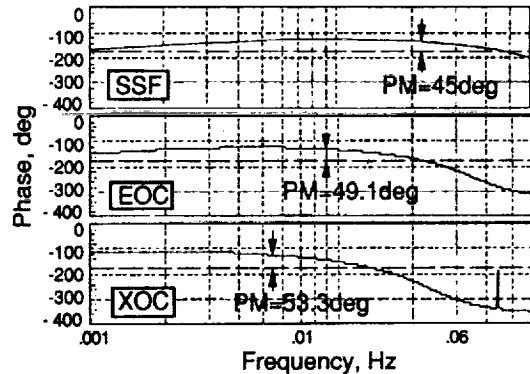

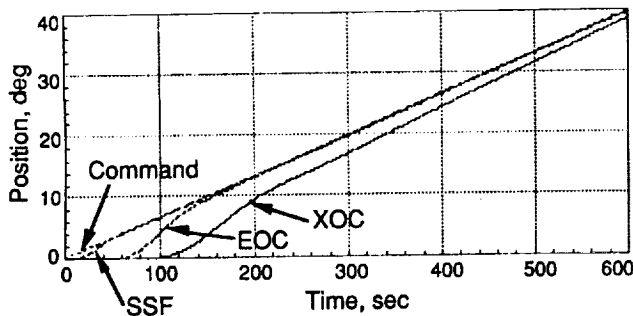Fig. 13 Comparison of compensated Bode phase plots of port velocity open loop

8

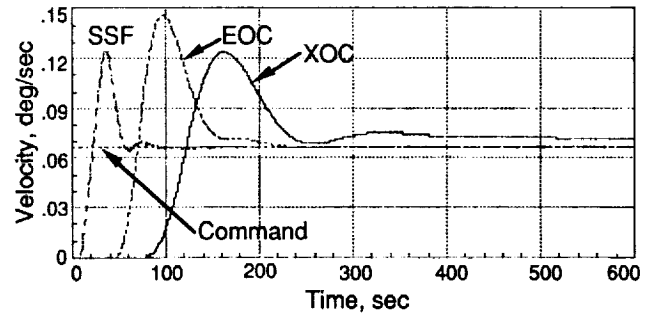Fig. 14 Comparison of position tracking

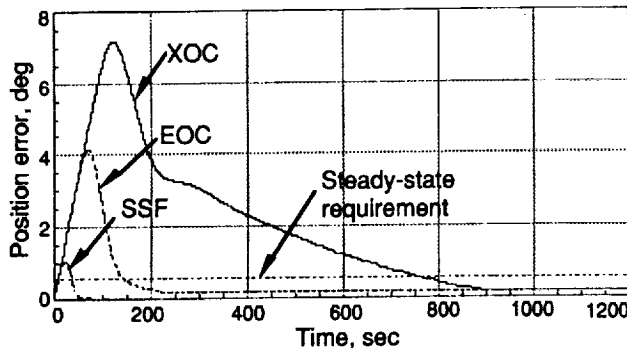Fig. 15 Comparison of velocity tracking
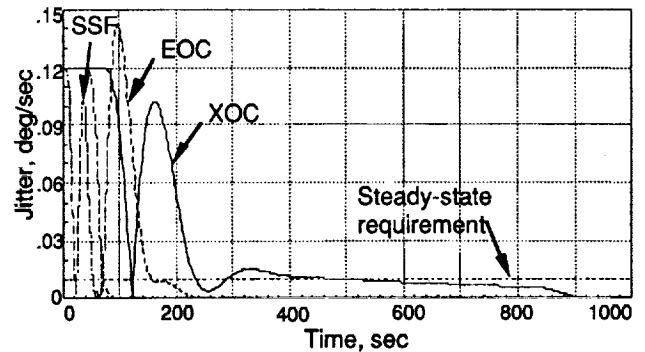

Fig. 16 Comparison of position tracking error

Fig. 17 Comparison of jitter

accounted in the simulation. The position command input and the resulting response are compared in Fig. 14. The velocity response to the command is shown in Fig. 15. After a brief initial transient period the tracking is performed accurately for SSF. However, due to the smaller bandwidths achieved for EOC and XOC, it takes longer for the tracking error to be eliminated. The position error, i.e., the difference between the position command and the actual position response, is shown in Fig. 16. The steady state pointing error, which should be less than 0.58 deg, is met within 40 sec, 150 sec and 760 sec for SSF, EOC and XOC, respectively. Jitter time history is shown in Fig. 17. The steady-state jitter requirement is met for all the configurations.

Figures 18 and 19 illustrate the torque generated by the motor to perform the Alpha Joint pointing and the net torque applied to the station after overcoming the friction. No net torque is applied to the station until the motor torque overcomes the static friction. Once the motion of the Alpha Joint is initiated, the dynamic friction comes into play and the magnitude of the steady-state motor torque is just enough to overcome the dynamic friction. As a result, the core structure of the station does not experience a net torque applied from the joint motor until after the initial transient period of 100 sec, 250 sec, and 400 sec for SSF, EOC, and XOC, respectively. The maximum torque available is approximately 30,000 in-lbf. The peak motor torque required is well within the torque limit. Therefore, the assumption that the motor is capable of producing the level of torque required by the synthesized design is verified.

The transient net torque applied on the outboard structure causes a reaction torque on the core structure. This reaction torque has to be compensated by RCS jet and CMG torques to maintain the attitude of the core structure. This paper assumes that the reaction torque is compensated ideally and the rigid body attitude of the core structure remains stationary. If a feathering maneuver using the Alpha Joint is required during each orbit to

reduce the drag, RCS jet firings are required since CMG's do not have sufficient control authority and momentum storage to provide attitude control of the core structure. A 25 lbf attitude control RCS jet firing is equivalent to 20 µg rigid body acceleration for the XOC configuration whose total weight on earth is approximately 1.2×10^6 lbf. Therefore, a microgravity level cannot be maintained during a feathering maneuver and the feathering maneuver for each orbit would require an excessive amount of RCS jet fuel.

Conclusions

This paper addressed the sun tracking control system design of the Solar Alpha Rotary Joint (SARJ) and the interaction of the control system with the flexible structures of Space Station Freedom (SSF) evolutionary concepts. The significant components of the space station configurations pertaining to the SARJ control were described and the tracking control system design was presented. Finite element models representing two evolutionary concepts, Enhanced Operations Capability (EOC) and Extended Operations Capability (XOC), were generated. Assuming that the SSF based solar tracking control system design and requirements are imposed on the space station evolutionary configurations, the influence of a low frequency flexible structure on the solar tracking control system performance was evaluated and how that influence limits the space station growth was explored. A procedure for synthesizing the values of the control system design variables was presented using a constrained optimization technique to meet design requirements, to provide a given level of control system stability margin, and to achieve the most responsive tracking performance. The synthesis procedure described in this study would be useful in designing tracking control systems of articulating large flexible structures whose dominant structural mode frequency is close to the control bandwidth.
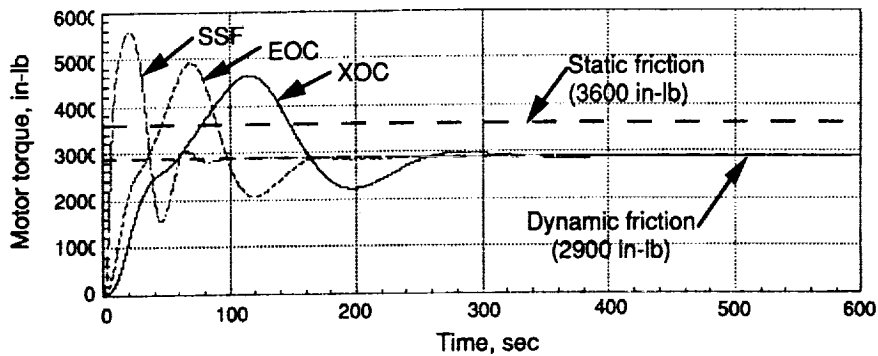
9

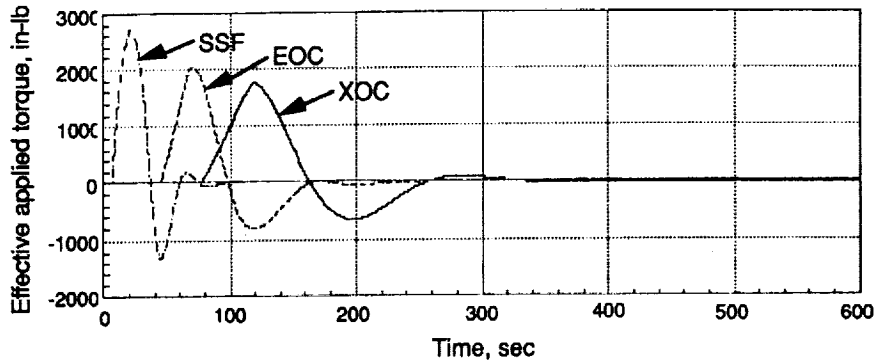Fig. 18 Comparison of motor torque

Fig. 19 Comparison of effective applied torque

Control/structure interaction was influenced by a limited number of dominant modes which were configuration dependent and not necessarily the lowest frequency modes. The dominant modes for SSF were characterized by the rigid body rotation of the outboard truss structure and bending of the photovoltaic array masts; whereas, the SSF evolutionary concepts exhibited dominant modes which were closer to the fundamental frequency and characterized by a combined bending and torsion of the transverse booms. The resulting control system design and performance for SSF, EOC, and XOC were compared. All design requirements were met except the bandwidth of XOC design. Due to the low frequency of the dominant XOC flexible mode, the SSF imposed minimum control bandwidth of 0.01 Hz was not achieved resulting in sluggish performance. If the SSF bandwidth requirement is enforced for XOC, the SSF Preliminary Design Review Alpha Joint controller design may not be acceptable. Revised controller design employing sophisticated control/structure interaction techniques may need to be investigated or a lower bandwidth controller must be accepted.

The level of control torque applied during the start-up tracking control period indicates that a feathering operation for each orbit to reduce the aerodynamic drag during the orbital night time may not be feasible. Since the Control Moment Gyros (CMG's) do not have enough control authority and the Reaction Control System (RCS) jet firings are required to maintain the attitude during the feathering operations in each orbit, the micro gravity environment would be disturbed and excessive amount of RCS jet fuel would be required.

References

1. Laskin, R. A, Estus, J. M., Lin, Y. H., Spanos, J. T., and Scatter, C. M., "NASA Office of Space Science and Applications Study on Space Station Attached Payload Pointing," AIAA Paper 88-4105, *Proceedings of AIAA Guidance, Navigation and Control Conference*, Minneapolis, MN, Aug. 1988, pp. 430-443.
2. Bone, J. and Nuttall, N., "Performance Assessment of the Solar Alpha Rotary Joint Control System with a Flexible Dynamic Load Model," EM-2-ME-014, PDR document MDC H6506, Work Package 2, June 1990.
3. Merritt, L. V., "Rotary Joint Servo Loops: General Description with Performance Models," Rough Draft of EM-2-ME-62, Lockheed Missiles & Space Company, Space Station Work Package 2, March 1990.
4. Merritt, L. V., "The Space Station Rotary Joint Motor Controller," *Motion Journal*, Jan./Feb. 1990, pp. 14-22.
5. Lam, H. Y-F., *Analog and Digital Filters: Design and Realization*, Prentice Hall, 1979, p. 301.
6. *MATRIXx Optimization Module Manual*, Edition 2, Integrated Systems, Inc., October 1989.
7. Kumar, R. R., Cooper, P. A., and Lim, T. W., "Sensitivity of Space Station Alpha Joint Robust Controller to Structural Modal Parameter Variations," AIAA Paper 91-2665, *Proceedings of AIAA Guidance, Navigation, and Control Conference*, New Orleans, LA, August 1991.

REPORT DOCUMENTATION PAGE

1. AGENCY USE ONLY (Leave blank)	2. REPORT DATE May 1992	3. REPORT TYPE AND DATES COVERED Technical Memorandum

4. TITLE AND SUBTITLE

Structural Dynamic Interaction with Solar Tracking Control for Evolutionary Space Station Concepts

5. FUNDING NUMBERS

WU 590-14-31-01

6. AUTHOR(S)

Tae W. Lim, Paul A. Cooper, and J. Kirk Ayers

7. PERFORMING ORGANIZATION NAME(S) AND ADDRESS(ES)

NASA Langley Research Center
Hampton, VA 23665-5225

8. PERFORMING ORGANIZATION REPORT NUMBER

9. SPONSORING/MONITORING AGENCY NAME(S) AND ADDRESS(ES)

National Aeronautics and Space Administration
Washington, DC 20546-0001

10. SPONSORING/MONITORING AGENCY REPORT NUMBER

NASA TM-107629

11. SUPPLEMENTARY NOTES

Lim: Lockheed Engineering & Sciences Co., Hampton, VA; Cooper:NASA Langley Research Center, Hampton, VA; Ayers: Lockheed Engineering & Sciences Co., Hampton, VA
Presented at the 33rd Structures, Structural Dynamics and Materials Conference, Dallas, TX, March 13-15, 1992

12a. DISTRIBUTION/AVAILABILITY STATEMENT

Unclassified--Unlimited

Subject Category 39

12b. DISTRIBUTION CODE

13. ABSTRACT (Maximum 200 words)

This paper addresses the sun tracking control system design of the Solar Alpha Rotary Joint (SARJ) and the interaction of the control system with the flexible structure of Space Station Freedom (SSF) evolutionary concepts. The significant components of the space station pertaining to the SARJ control are described and the tracking control system design is presented. Finite element models representing two evolutionary concepts, Enhanced Operations Capability (EOC) and Extended Operations Capability (XOC), are employed to evaluate the influence of low frequency flexible structure on the control system design and performance. The design variables of the control system are synthesized using a constrained optimization technique to meet design requirements, to provide a given level of control system stability margin, and to achieve the most responsive tracking performance. The resulting SARJ control system desugn and performance of the EOC and XOC configurations are presented and compared to those of the SSF configuration. Performance limitations caused by the low frequency of the dominant flexible mode are discussed.

14. SUBJECT TERMS

Solar Tracking Control, Evolutionary Space Station Concepts, Controls-Structures Interaction

15. NUMBER OF PAGES

11

16. PRICE CODE

A03

17. SECURITY CLASSIFICATION OF REPORT	18. SECURITY CLASSIFICATION OF THIS PAGE	19. SECURITY CLASSIFICATION OF ABSTRACT	20. LIMITATION OF ABSTRACT
Unclassified	Unclassified		